Dynamical Topological Transitions in the Massive Schwinger Model with a θ Term

T. V. Zache,[1,*] N. Mueller,[2] J. T. Schneider,[1] F. Jendrzejewski,[3] J. Berges,[1] and P. Hauke[1,3]
[1]Heidelberg University, Institut für Theoretische Physik, Philosophenweg 16, 69120 Heidelberg, Germany
[2]Physics Department, Brookhaven National Laboratory, Building 510A, Upton, New York 11973, USA
[3]Heidelberg University, Kirchhoff-Institut für Physik, Im Neuenheimer Feld 227, 69120 Heidelberg, Germany

(Received 27 August 2018; revised manuscript received 17 December 2018; published 6 February 2019)

Aiming at a better understanding of anomalous and topological effects in gauge theories out of equilibrium, we study the real-time dynamics of a prototype model for CP violation, the massive Schwinger model with a θ term. We identify dynamical quantum phase transitions between different topological sectors that appear after sufficiently strong quenches of the θ parameter. Moreover, we establish a general dynamical topological order parameter, which can be accessed through fermion two-point correlators and, importantly, which can be applied for interacting theories. Enabled by this result, we show that the topological transitions persist beyond the weak-coupling regime. Finally, these effects can be observed with tabletop experiments based on existing cold-atom, superconducting-qubit, and trapped-ion technology. Our Letter thus presents a significant step towards quantum simulating topological and anomalous real-time phenomena relevant to nuclear and high-energy physics.

DOI: 10.1103/PhysRevLett.122.050403

Introduction.—The topological structure of gauge theories has many important manifestations [1–5]. In quantum chromodynamics (QCD), e.g., it allows for an additional term in the action that explicitly breaks charge conjugation parity (CP) symmetry [6–8]. Though the angle θ that parametrizes this term is in principle unconstrained, experiments have found very strong bounds on CP violation, consistent with $\theta = 0$ [9]. In one elegant explanation, θ is described as a dynamical field that undergoes a phase transition, the "axion" [10–12], which is currently sought after in experiments [13]. However, the controlled study of topological effects far from equilibrium remains highly challenging [14]. So-called quantum simulators offer an attractive alternative approach. These are engineered quantum devices that mimic desired Hamiltonians in an analog way or synthesize them on digital (qubit-based) quantum computers [15–17]. While theories of the standard model, such as QCD, are beyond the current abilities of quantum simulators, existing technology [18,19] can already simulate simpler models, which puts insight into the topological properties of gauge theories within reach. In this respect, the massive Schwinger model [20], describing quantum electrodynamics (QED) in $1+1$ dimensions, is particularly interesting because it allows for a CP-odd θ term similar to QCD. However, while ground-state and thermal properties of QCD and of the Schwinger model have been extensively studied [21,22], much less is known about their topological structure out of equilibrium.

In this Letter, we investigate the nonequilibrium real-time evolution of the massive Schwinger model after a quench of the topological θ angle. We find topological transitions in the fermion sector, which appear as vortices in the single-particle propagator when θ changes by more than a critical value. In the limit of vanishing gauge coupling, we rigorously connect this phenomenon to dynamical quantum phase transitions (DQPTs), which in condensed-matter lattice models are currently receiving considerable attention [23–26]. A topological nature of DQPTs has previously been revealed in noninteracting theories [27–29]. Here, we demonstrate how to construct a general dynamical topological invariant that is valid in the continuum and, most importantly, also in interacting theories. Moreover, our topological invariant provides a physical interpretation of DQPTs in terms of fermionic correlation functions. Enabled by this result, we use nonperturbative real-time lattice calculations at intermediate to strong coupling to show that the topological transition persists up to $e/m \lesssim 1$. Already for lattices as small as eight sites, we obtain good infrared convergence. Moreover, the relevant phenomena occur on timescales that have already been accessed in proof-of-principle quantum simulations of gauge theories [18,19]. These features will enable near-future experiments based on trapped ions [18], superconducting qubits [19], and cold neutral atoms [30] to probe this dynamical topological transition.

θ quenches in the massive Schwinger model.—The massive Schwinger model is a prototype model for $3+1$D QCD since both share important features, such as a nontrivial topological vacuum structure and a chiral anomaly [20,21]. CP violation can be studied by adding a so-called topological θ term $(e\theta/2\pi)E_x$ to the Hamiltonian density, where E is the electric field and e is the dimensionful gauge coupling. In the temporal axial gauge, and by making a chiral transformation, the θ term can be absorbed

into the fermion mass term to give the following Hamiltonian [20]:

$$H_\theta = \int dx \left[\frac{1}{2}E_x^2 + \psi_x^\dagger \gamma^0 (i\gamma^1 D_x + m e^{i\theta\gamma^5})\psi_x\right]. \quad (1)$$

Here, ψ are two-component fermion operators, $\gamma^{0/1}$ constitute a two-dimensional Clifford algebra, and $\gamma^5 \equiv \gamma^0\gamma^1$. The Hamiltonian contains the energy of the electric field, the kinetic term of the fermions, which are coupled to the gauge sector via the covariant derivative $D_x = \partial_x + ieA_x$, where e is the electric coupling, and the fermion rest mass m. While the addition of the θ term is an imaginary contribution to the action (see, e.g., [31]), we emphasize that the Hamiltonian (1) remains Hermitian. In particular, its spectrum is real and θ does not introduce any instability.

Here, we wish to study how topological properties appearing through the CP-violating θ term become manifest in the real-time dynamics of the theory. To this end, we prepare the system in the ground state $|\Omega(\theta)\rangle$ of H_θ and switch abruptly to another value θ', thereby quenching the system out of equilibrium. Since the θ angle in the massive Schwinger model has the same topological origin as its counterpart in $3+1$D QCD, we can interpret the studied quench as a classical external axion field. In the following, we will show that this quench generates topological transitions, which appear as momentum-time vortices in the phase of the gauge-invariant time-ordered Green's function,

$$g_{\theta\to\theta'}(k,t) = \int dx e^{-ikx} \langle \psi^\dagger(x,t) e^{-ie\int_0^x dx' A(x',t)} \psi(0,0)\rangle. \quad (2)$$

Here, we abbreviated $\langle\cdots\rangle = \langle\Omega(\theta)|\cdots|\Omega(\theta)\rangle$ and $O(x,t) = e^{iH_{\theta'}t}O(x)e^{-iH_{\theta'}t}$ with $O \in \{\psi, \psi^\dagger, A\}$, which encodes the dependence on the quench parameters. We will first discuss these topological transitions in the continuum theory at weak coupling, where we show analytically their direct correspondence to DQPTs. These results will motivate the definition of a general topological invariant, which will enable us to study also the interacting theory, discussed further below.

Weak-coupling limit.—In the weak-coupling limit, $e/m \to 0$, the massive Schwinger model is a free fermionic theory that can be solved analytically by diagonalizing $H_\theta = \int dk H_\theta(k)$, with $H_\theta(k) = \psi_k^\dagger \gamma^0 (k\gamma^1 + m e^{i\theta\gamma^5})\psi_k$. Figure 1 displays the phase of $g_{\theta\to\theta'}$ as a function of (k,t) for two exemplary quenches with $\Delta\theta = 0.45\pi, \pi$ [our results here depend only on $\Delta\theta = (\theta - \theta') \in (-\pi, \pi]$]. Strong quenches in the range $|\Delta\theta| > (\pi/2)$ are accompanied by the formation of vortices at critical times $t_c^{(n)} = (2n-1)t_c$, with $t_c = \pi/[2\omega(k_c)]$, $n \in \mathbb{N}$, and $\omega(k) = \sqrt{k^2+m^2}$. These appear in pairs of opposite winding at critical modes $\pm k_c = \pm m\sqrt{-\cos(\Delta\theta)}$.

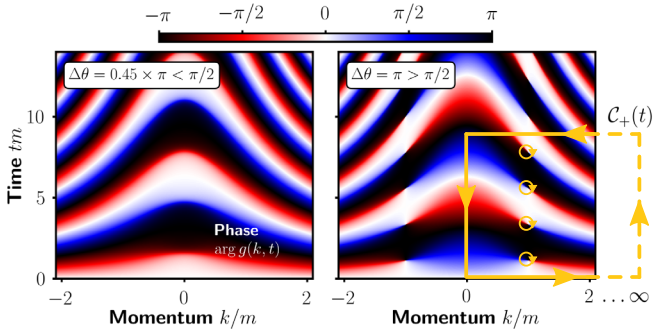

FIG. 1. Phase of the time-ordered correlator [Eq. (2)] after θ quenches at vanishing gauge coupling. The real-time evolution of the phase exhibits qualitative differences when the quench is weaker or stronger than the critical value $\Delta\theta_c = \pi/2$, exemplified here for $\Delta\theta = 0.45\pi$ (left) and $\Delta\theta = \pi$ (right). The phase is analytic for small quenches ($|\Delta\theta| < \Delta\theta_c$), while for large quenches ($|\Delta\theta| > \Delta\theta_c$) vortices form at $(\pm k_c, t_c^{(n)})$. The integration path $\mathcal{C}_+(t)$, here shown for $tm \approx 9$, encloses a discrete number of vortices (marked by yellow circles), leading to integer increments of the topological invariant ν as time progresses (see Fig. 2).

This observation suggests to define a dynamical topological order parameter that counts the difference of vortices contained in left ($-$) vs right ($+$) moving modes, $\nu \equiv n_+ - n_-$, with

$$n_\pm(t) \equiv \frac{1}{2\pi}\oint_{\mathcal{C}_\pm(t)} d\mathbf{z}\{\tilde{g}^\dagger(\mathbf{z})\nabla_{\mathbf{z}}\tilde{g}(\mathbf{z})\}. \quad (3)$$

Here, $\tilde{g}(\mathbf{z}) \equiv g_{\theta\to\theta'}(k,t')/|g_{\theta\to\theta'}(k,t')|$ and $\mathcal{C}_\pm(t)$ is a rectangular path enclosing the left or right half of the $\mathbf{z} = (k,t')$ plane up to the present time t; i.e., it runs (counterclockwise) along $(0,0) \leftrightarrow (0,t) \leftrightarrow (\pm\infty, t) \leftrightarrow (\pm\infty, 0) \leftrightarrow (0,0)$ as visualized in Fig. 1. As exemplified in Fig. 2(a), the topological invariant remains trivial for $|\Delta\theta| < \pi/2$, while for $|\Delta\theta| > \pi/2$ it changes abruptly at critical times $t_c^{(n)}$.

These critical times coincide with fundamental changes in the properties of the real-time evolution, coined DQPTs [23]. DQPTs are revealed in the so-called Loschmidt amplitude, which is related to the vacuum persistence amplitude [32] and which is a common measure, e.g., in the field of quantum chaos [33]. The Loschmidt amplitude quantifies the overlap of the time-evolved state with its initial condition

$$L_{\theta\to\theta'}(t) \equiv \langle\Omega(\theta)|e^{-iH_{\theta'}t}|\Omega(\theta)\rangle. \quad (4)$$

It is convenient to further define an intensive "rate function"

$$\Gamma^{(L)}_{\theta\to\theta'}(t) \equiv -\lim_{V\to\infty}\frac{1}{V}\log|L_{\theta\to\theta'}(t)|. \quad (5)$$

DQPTs appear as nonanalyticities of Eq. (5) [zeros of Eq. (4)].

In the limit $e/m \to 0$, where the system is in a product state $|\Omega(\theta)\rangle = \bigotimes_k |\Omega_k(\theta)\rangle$, the Loschmidt amplitude can be decomposed into Fourier modes,

$$L_{\theta\to\theta'}(t) = \prod_k \langle\Omega_k(\theta)|e^{-iH_{\theta'}(k)t}|\Omega_k(\theta)\rangle. \tag{6}$$

At $e/m \to 0$, we have the additional identity $\langle\Omega_k(\theta)|e^{-iH_{\theta'}(k)t}|\Omega_k(\theta)\rangle = g_{\theta\to\theta'}(k,t)$. Thus, zeros of the Loschmidt amplitude imply that the phase of the Green's function becomes undefined for a critical mode, enabling the appearance of the vortices seen in Fig. 1. As a consequence, at zero coupling the topological transitions and nonanalyticities of the rate function in Eq. (5) strictly coincide [see Fig. 2(b)].

For noninteracting lattice theories, a topological nature of DQPTs has previously been revealed through the phase of the Fourier-decomposed Loschmidt amplitude, $\arg[\langle\Omega_k(\theta)|\exp[-iH_{\theta'}(k)t]|\Omega_k(\theta)\rangle] = \phi_{\text{geom}} + \phi_{\text{dyn}}$ [27]. Here, the total phase has been divided into a trivial dynamical phase $\phi_{\text{dyn}}(k,t)$ and the so-called Pancharatnam geometric phase $\phi_{\text{geom}}(k,t)$. At a DQPT, the winding number of ϕ_{geom} changes by an integer. This change can be computed by integration across (half) the Brillouin zone at fixed time t [27], which has been used in the recent experiments of Refs. [28,29]. For this prescription to work, however, one needs to subtract the trivial dynamical phase ϕ_{dyn}, which can reasonably be obtained only perturbatively close to the noninteracting case. Compared to this standard prescription, our construction in Eq. (3) has a number of advantages. First, the prescription of Ref. [27] fails for $\theta \neq 0, \pi$, where the absence of a particle-hole symmetry makes modes at $k = 0, \pm\infty$ inequivalent. Second, and more importantly, by using a closed path in the (k,t) plane (cf. Fig. 1) only the singular geometric part contributes to the integral in Eq. (3), irrespective of the smooth dynamical phase. Thus, together with the definition through fermionic correlators [Eq. (2)], instead of Fourier modes of the wave function overlap [Eq. (6)], our formulation enables us to tackle also the interacting theory.

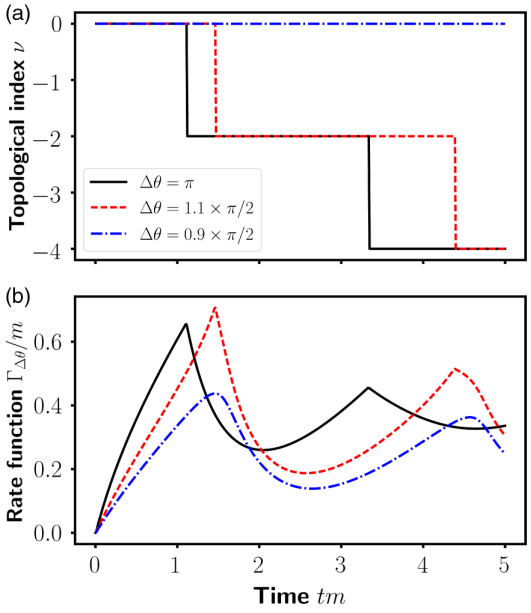

FIG. 2. Dynamical topological transitions at vanishing gauge coupling. (a) The topological invariant exhibits jumps at critical times $t_c^{(n)} = (2n-1)\pi/[2\omega(k_c)]$ with $n \in \mathbb{N}$, if $|\Delta\theta| > \pi/2$, while the dynamics is topologically trivial for $|\Delta\theta| < \pi/2$. (b) For $|\Delta\theta| > \pi/2$, the rate function [Eq. (5)] shows nonanalytic kinks at times $t_c^{(n)}$.

Towards strong coupling.—To investigate if the topological transitions persist at nonvanishing coupling, $e/m > 0$, we perform nonperturbative real-time lattice simulations based on exact diagonalization (ED), using the PYTHON package QUSPIN [34]. We focus on the strongest quench $\Delta\theta = \pi$ (or $-m \to m$), using staggered fermions with lattice Hamiltonian [35]

$$\frac{H}{a} = \sum_{n=0}^{N-1}\left[\frac{E_n^2}{2} + m(-1)^n\phi_n^\dagger\phi_n - \frac{i}{2a}(\phi_n^\dagger U_n\phi_{n+1} - \text{H.c.})\right]. \tag{7}$$

Here, ϕ_n are one-component fermion operators on an even number of lattice sites N, E_n and U_n are electric fields and links, and a is the lattice spacing. To apply ED, we restrict the simulation to the physical Hilbert space by solving the Gauss law constraint $G_n|\text{phys}\rangle = 0$ with $G_n = E_n - E_{n-1} - e\{\phi_n^\dagger\phi_n + [(-1)^n - 1/2]\}$. In contrast to previous works [18,36], we use periodic boundary conditions [37] (see [38] for more details). To efficiently compute the topological invariant ν in our numerics, we adapt a formalism that has originally been developed for computing Chern numbers in momentum space [39]. The possibility to adapt this formalism to our case is another feature of our definition in Eq. (3) since it is enabled by the use of a closed integration path in the (k,t) plane. This adaption forces ν to remain integer valued even when evaluated on coarse grids, thus leading to convergence already for small lattices [40].

As can be expected from the above discussions, at small e/m transitions in the topological invariant coincide with maxima in the rate function (see Fig. 3). Further, both structures congruently persists at larger values of e/m. Importantly, however, while the system sizes accessible for ED do not allow one to discern clear kinks in the rate function, the nonequilibrium topological invariant ν sharply distinguishes between topologically inequivalent phases, revealing a shift of the transitions towards larger t_c as e/m

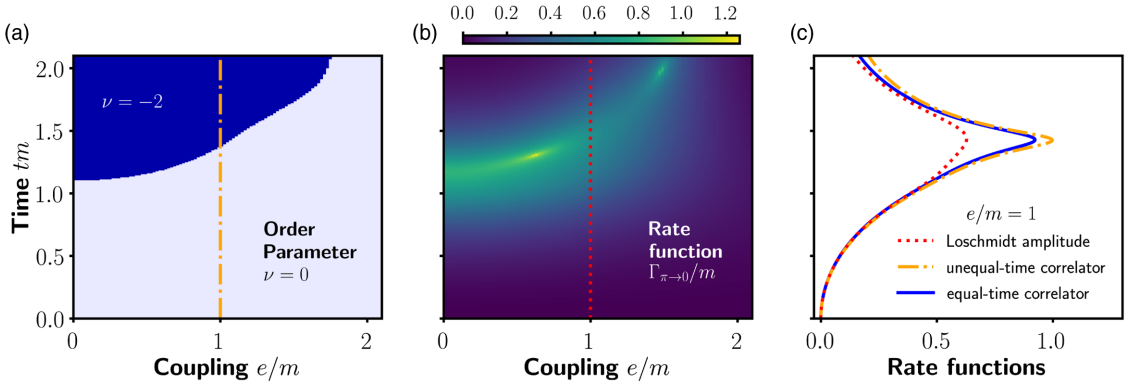

FIG. 3. Dynamical topological transitions beyond weak coupling. (a) The integer-valued topological invariant ν clearly distinguishes different "phases" in the (t, e) plane. The topological transition persists at larger coupling, but shifts towards later times and appears at sufficiently large coupling. (b) The maxima of the rate function obtained from the many-body overlap agree qualitatively with the transitions in ν, but are blurred by the finite lattice size. (c) Rate functions computed from the full wave function overlap [red dotted line; cf. (b) and Eq. (5)], from fermionic two-time correlators [orange dot-dashed line; cf. (a) and Eq. (2)], and equal-time correlators [blue solid line; cf. Eq. (8)] all indicate the same time of the first topological transition, here illustrated for $e/m = 1$. Simulations are for a small lattice of $N = 8$ sites, as relevant for first quantum-simulator experiments, and with lattice spacing $am = 0.8$.

is increased. While the results for $e/m \lesssim 1$ are already reasonably finite-volume converged for the small system size plotted, at $e/m \gtrsim 1$ finite-volume effects persist up to $N = 20$ (cf. [38] and the Supplemental Material [41]). Nevertheless, the topological transition must vanish at sufficiently large coupling e_c because θ becomes an irrelevant parameter in the limit $m \to 0$ [42]. Finite-size effects in our numerical results hinder a quantitative determination of e_c. Motivated by these limitations, we propose a possible quantum simulation of the present setup.

Quantum simulation.—Importantly, the first topological transition happens on times of order $t_c m \sim 1$–2, which lies within coherence times that are accessible with existing and proposed quantum simulators [18,19,30]. A straightforward realization of the scenario discussed in this Letter may be achieved with a quantum computer based on trapped ions or superconducting qubits, where quench dynamics has been studied recently [18,19]. Though these experiments used only four lattice sites of staggered fermions, larger lattices are within reach of current technology [43–46]. Very recently, it has been shown that variational algorithms can prepare the ground state of the lattice Schwinger model with 8–20 sites with high fidelity [47,48]. The relevant dynamics can be implemented by discretizing the unitary evolution operator into a sequence of quantum gates [18,49]. For staggered fermions, the mass term is realized by local rotations and can be quenched by inverting the direction of rotation. All observables studied in this Letter can then be accessed by an appropriate sequence of unitary operators intermitted by spin flips. Alternatively, various works have proposed analog quantum simulators of the massive Schwinger model [50–53]. One possible implementation is based on a mixture of bosonic and fermionic atoms in a tilted optical lattice [30], where the fermion mass corresponds to Rabi oscillations between two hyperfine states driven by radio frequency radiation. In this setup, a mass quench may be simply implemented by abruptly adjusting the corresponding Rabi frequency.

These experiments may unveil the topological transitions through different observables: First, a digital quantum computer could, in principle, work with the many-body wave functions to directly calculate the order parameter ν [Eq. (3)] and the rate function $\Gamma_{\theta\to\theta'}(t)$ [Eq. (5)]. Second, one could measure the two-time correlator $g_{\theta\to\theta'}(k,t)$ [Eq. (2)] [54,55] and thereby avoid the study of many-body overlaps. Third, the discrete transition points of the order parameter are indicated also in experimentally more accessible equal-time correlation functions, $[\underline{F}(t)]^{\alpha\beta}_{xy} \equiv \langle[\psi^\alpha(t,x), \bar{\psi}^\beta(t,y)]\rangle$. Namely, let us define

$$K_{\theta\to\theta'}(t) \equiv \prod_k [\mathbf{F}(k,t) + \mathbf{F}(k,0)]^2, \tag{8}$$

where $\mathbf{F} = (F_s, F_1, F_5)$ are Lorentz components of the correlator, $\underline{F}(t) = F_s(t)\mathbf{1} + F_\mu(t)\gamma^\mu + iF_5(t)\gamma^5$ [56]. In the weak-coupling limit, one has $K_{\theta\to\theta'}(t) = \prod_k |g_{\theta\to\theta'}(k,t)|^2 = |L_{\theta\to\theta'}(t)|^2$ (for details, see [38]). This motivates us to define the rate functions $\Gamma^{(g)}(t)$ and $\Gamma^{(K)}(t)$ analogously to $\Gamma^{(L)}(t)$ by replacing $|L(t)|$ in Eq. (5) with $\prod_k |g(k,t)|$ and $\sqrt{K(t)}$, respectively. We thus have three complementary definitions that coincide for $e/m \to 0$, obtained from equal-time correlators [Eq. (8)], two-time correlators [Eq. (2)], and the full many-body Loschmidt amplitude [Eq. (4)]. Remarkably, as illustrated in Fig. 3(c) for $e/m = 1$, even at intermediate couplings the maxima of all three rate functions indicate the same critical times with relative deviation less than about 8%. See the Supplemental Material [41] for a quantitative comparison, which

demonstrates that the three rate functions show comparable finite-size deviations, which for the topological order parameter are significantly smaller.

Besides its experimental simplicity, Eq. (8) also gives an interesting interpretation of the dynamical topological transition in terms of a dephasing effect. Namely, Eq. (8) has zeros if and only if the mode k_c at time t_c exhibits perfect anticorrelation with the initial state, $\mathbf{F}(k_c, t_c) = -\mathbf{F}(k_c, 0)$. This anticorrelation is responsible for the nonanalytic behavior of the associated rate function.

Conclusions.—In this Letter, we have studied the real-time dynamics of massive $1 + 1$D QED with a θ term, as a prototype model for topological effects in gauge theories. By establishing a general dynamical topological order parameter, which can be obtained from fermionic correlators and is valid in interacting theories, we have identified the appearance of dynamical topological transitions after changes in the external axion field. A connection between the topological transitions to DQPTs, which is rigorous at zero coupling, persists in our numerics of the interacting theory, thus providing a physical interpretation of DQPTs in terms of fermionic correlators. Finally, our topological order parameter can directly be applied also in the study of condensed-matter models, where the construction of topological invariants for interacting systems is a major outstanding challenge [57–59].

In our Letter, we have identified a relevant problem for state-of-the-art quantum simulation. The described dynamical transitions constitute an ideal first step because the relevant dynamics appears at short timescales and small system sizes. We expect the topological nature to provide robustness against experimental imperfections, which may provide a starting point to tackle the question of certifiability of quantum simulation.

Despite the simplicity of the considered model, our study shows that quantum simulators provide a unique perspective to the topological structure of QCD out of equilibrium. Phenomena closely related to the physics studied in this Letter are the conjectured chiral magnetic and similar effects [60–63], which remain challenging in and out of equilibrium for theoretical studies [14,64–72]. Here, a simple next step for future quantum simulators is to model these effects by spatial domains of the θ parameter [73].

This work is part of and supported by the DFG Collaborative Research Centre "SFB 1225 (ISOQUANT)," the ERC Advanced Grant "EntangleGen" (Project No. 694561), and the Excellence Initiative of the German federal government and the state governments–funding line Institutional Strategy (Zukunftskonzept): DFG Project No. ZUK 49/Ü. N. M. is supported by the U.S. Department of Energy, Office of Science, Office of Nuclear Physics, under Award No. DE-SC0012704 and by the Deutsche Forschungsgemeinschaft (DFG, German Research Foundation) - Project No. 404640738.

Note added.—For a related work on dynamical quantum phase transitions in lattice gauge theories, see the article published on the arXiv on the same day by Huang *et al.* [74].

*zache@thphys.uni-heidelberg.de

[1] F. R. Klinkhamer and N. S. Manton, Phys. Rev. D **30**, 2212 (1984).
[2] R. F. Dashen, B. Hasslacher, and A. Neveu, Phys. Rev. D **10**, 4138 (1974).
[3] V. Soni, Phys. Lett. **93B**, 101 (1980).
[4] J. Boguta, Phys. Rev. Lett. **50**, 148 (1983).
[5] P. Forgacs and Z. Horvath, Phys. Lett. **138B**, 397 (1984).
[6] G. 't Hooft, Phys. Rev. D **14**, 3432 (1976).
[7] R. Jackiw and C. Rebbi, Phys. Rev. Lett. **37**, 172 (1976).
[8] C. G. Callan, Jr., R. F. Dashen, and D. J. Gross, Phys. Rev. D **20**, 3279 (1979).
[9] T. Chupp, P. Fierlinger, M. Ramsey-Musolf, and J. Singh, Rev. Mod. Phys. **91**, 015001 (2019).
[10] S. Weinberg, Phys. Rev. Lett. **40**, 223 (1978).
[11] F. Wilczek, Phys. Rev. Lett. **40**, 279 (1978).
[12] R. D. Peccei and H. R. Quinn, Phys. Rev. Lett. **38**, 1440 (1977).
[13] P. W. Graham, I. G. Irastorza, S. K. Lamoreaux, A. Lindner, and K. A. van Bibber, Annu. Rev. Nucl. Part. Sci. **65**, 485 (2015).
[14] M. Mace, S. Schlichting, and R. Venugopalan, Phys. Rev. D **93**, 074036 (2016).
[15] J. I. Cirac and P. Zoller, Nat. Phys. **8**, 264 (2012).
[16] P. Hauke, F. M. Cucchietti, L. Tagliacozzo, I. Deutsch, and M. Lewenstein, Rep. Prog. Phys. **75**, 082401 (2012).
[17] J. Carlson, D. Dean, M. Hjorth-Jensen, D. Kaplan, J. Preskill, K. Roche, M. Savage, and M. Troyer, Institute for Nuclear Theory Report No. 18-008, 2018.
[18] E. A. Martinez, C. A. Muschik, P. Schindler, D. Nigg, A. Erhard, M. Heyl, P. Hauke, M. Dalmonte, T. Monz, P. Zoller *et al.*, Nature (London) **534**, 516 (2016).
[19] N. Klco, E. Dumitrescu, A. McCaskey, T. Morris, R. Pooser, M. Sanz, E. Solano, P. Lougovski, and M. Savage, Phys. Rev. A **98**, 032331 (2018).
[20] S. R. Coleman, Ann. Phys. (N.Y.) **101**, 239 (1976).
[21] S. Coleman, R. Jackiw, and L. Susskind, Ann. Phys. (N.Y.) **93**, 267 (1975).
[22] P. Petreczky, J. Phys. G **39**, 093002 (2012).
[23] M. Heyl, A. Polkovnikov, and S. Kehrein, Phys. Rev. Lett. **110**, 135704 (2013).
[24] N. Fläschner, D. Vogel, M. Tarnowski, B. S. Rem, D.-S. Lühmann, M. Heyl, J. C. Budich, L. Mathey, K. Sengstock, and C. Weitenberg, Nat. Phys. **14**, 265 (2018).
[25] P. Jurcevic, H. Shen, P. Hauke, C. Maier, T. Brydges, C. Hempel, B. P. Lanyon, M. Heyl, R. Blatt, and C. F. Roos, Phys. Rev. Lett. **119**, 080501 (2017).
[26] M. Heyl, Rep. Prog. Phys. **81**, 054001 (2018).
[27] J. C. Budich and M. Heyl, Phys. Rev. B **93**, 085416 (2016).
[28] T. Tian, Y. Ke, L. Zhang, S. Lin, Z. Shi, P. Huang, C. Lee, and J. Du, arXiv:1807.04483.

[29] X.-Y. Xu, Q.-Q. Wang, M. Heyl, J. C. Budich, W.-W. Pan, Z. Chen, M. Jan, K. Sun, J.-S. Xu, Y.-J. Han *et al.*, arXiv:1808.03930.

[30] T. V. Zache, F. Hebenstreit, F. Jendrzejewski, M. K. Oberthaler, J. Berges, and P. Hauke, Quantum Sci. Technol. **3**, 034010 (2018).

[31] Y. Shimizu and Y. Kuramashi, Phys. Rev. D **90**, 074503 (2014).

[32] F. Gelis and N. Tanji, Prog. Part. Nucl. Phys. **87**, 1 (2016).

[33] T. Gorin, T. Prosen, T. H. Seligman, and M. Žnidarič, Phys. Rep. **435**, 33 (2006).

[34] P. Weinberg and M. Bukov, arXiv:1804.06782.

[35] T. Banks, L. Susskind, and J. B. Kogut, Phys. Rev. D **13**, 1043 (1976).

[36] C. J. Hamer, Z. Weihong, and J. Oitmaa, Phys. Rev. D **56**, 55 (1997).

[37] To obtain a finite-dimensional Hilbert space, we drop the single remaining bosonic mode describing a constant background field.

[38] T. V. Zache *et al.* (to be published).

[39] T. Fukui, Y. Hatsugai, and H. Suzuki, J. Phys. Soc. Jpn. **74**, 1674 (2005).

[40] In the noninteracting limit, the topological invariant is not affected by the choice of lattice regularization, which we have explicitly checked at the example of staggered and Wilson fermions. In this Letter, we restrict the simulations in the interacting case to staggered fermions and further details will be presented in a subsequent extended study [38].

[41] See Supplemental Material at http://link.aps.org/supplemental/10.1103/PhysRevLett.122.050403 for a quantitative comparison of the transition times indicated by the topological order parameter and the rate functions.

[42] E. Abdalla, M. C. B. Abdalla, and K. D. Rothe, *Non-Perturbative Methods in 2 Dimensional Quantum Field Theory* (World Scientific, Singapore, 1991).

[43] T. Monz, D. Nigg, E. A. Martinez, M. F. Brandl, P. Schindler, R. Rines, S. X. Wang, I. L. Chuang, and R. Blatt, Science **351**, 1068 (2016).

[44] R. Barends, A. Shabani, L. Lamata, J. Kelly, A. Mezzacapo, U. Las Heras, R. Babbush, A. G. Fowler, B. Campbell, Y. Chen *et al.*, Nature (London) **534**, 222 (2016).

[45] A. Kandala, A. Mezzacapo, K. Temme, M. Takita, M. Brink, J. M. Chow, and J. M. Gambetta, Nature (London) **549**, 242 (2017).

[46] K. A. Landsman, C. Figgatt, T. Schuster, N. M. Linke, B. Yoshida, N. Y. Yao, and C. Monroe, arXiv:1806.02807.

[47] C. Kokail, C. Maier, R. van Bijnen, T. Brydges, M. K. Joshi, P. Jurcevic, C. A. Muschik, P. Silvi, R. Blatt, C. F. Roos *et al.*, arXiv:1810.03421.

[48] H.-H. Lu, N. Klco, J. M. Lukens, T. D. Morris, A. Bansal, A. Ekström, G. Hagen, T. Papenbrock, A. M. Weiner, M. J. Savage *et al.*, arXiv:1810.03959.

[49] C. Muschik, M. Heyl, E. Martinez, T. Monz, P. Schindler, B. Vogell, M. Dalmonte, P. Hauke, R. Blatt, and P. Zoller, New J. Phys. **19**, 103020 (2017).

[50] U.-J. Wiese, Ann. Phys. (Amsterdam) **525**, 777 (2013).

[51] E. Zohar, J. I. Cirac, and B. Reznik, Rep. Prog. Phys. **79**, 014401 (2016).

[52] M. Dalmonte and S. Montangero, Contemp. Phys. **57**, 388 (2016).

[53] G. Magnifico, D. Vodola, E. Ercolessi, S. P. Kumar, M. Müller, and A. Bermudez, Phys. Rev. D **99**, 014503 (2019).

[54] M. Knap, A. Kantian, T. Giamarchi, I. Bloch, M. D. Lukin, and E. Demler, Phys. Rev. Lett. **111**, 147205 (2013).

[55] P. Uhrich, C. Gross, and M. Kastner, Quantum Sci. Technol. **4**, 024005 (2019).

[56] We exclude F_0 in $\mathbf{F}$ because modewise charge conservation implies $F_0(k,t) = 0$ at $e/m = 0$.

[57] V. Gurarie, Phys. Rev. B **83**, 085426 (2011).

[58] N. Goldman, J. Budich, and P. Zoller, Nat. Phys. **12**, 639 (2016).

[59] S. Rachel, Rep. Prog. Phys. **81**, 116501 (2018).

[60] D. E. Kharzeev, L. D. McLerran, and H. J. Warringa, Nucl. Phys. **A803**, 227 (2008).

[61] K. Fukushima, D. E. Kharzeev, and H. J. Warringa, Phys. Rev. D **78**, 074033 (2008).

[62] D. E. Kharzeev, J. Liao, S. A. Voloshin, and G. Wang, Prog. Part. Nucl. Phys. **88**, 1 (2016).

[63] V. Koch, S. Schlichting, V. Skokov, P. Sorensen, J. Thomas, S. Voloshin, G. Wang, and H.-U. Yee, Chin. Phys. C **41**, 072001 (2017).

[64] D. T. Son and P. Surowka, Phys. Rev. Lett. **103**, 191601 (2009).

[65] H.-U. Yee, J. High Energy Phys. 11 (2009) 085.

[66] D. T. Son and N. Yamamoto, Phys. Rev. Lett. **109**, 181602 (2012).

[67] M. A. Stephanov and Y. Yin, Phys. Rev. Lett. **109**, 162001 (2012).

[68] J.-W. Chen, J.-y. Pang, S. Pu, and Q. Wang, Phys. Rev. D **89**, 094003 (2014).

[69] N. Müller, S. Schlichting, and S. Sharma, Phys. Rev. Lett. **117**, 142301 (2016).

[70] M. Mace, N. Mueller, S. Schlichting, and S. Sharma, Phys. Rev. D **95**, 036023 (2017).

[71] N. Mueller and R. Venugopalan, Phys. Rev. D **97**, 051901 (2018).

[72] N. Mueller and R. Venugopalan, Phys. Rev. D **96**, 016023 (2017).

[73] K. Tuchin, Phys. Rev. C **97**, 064914 (2018).

[74] Y. P. Huang, D. Banerjee, and M. Heyl, arXiv:1808.07874.